Polyhedron 60 (2013) 39–46

Contents lists available at SciVerse ScienceDirect

Polyhedron

journal homepage: www.elsevier.com/locate/poly

Structural studies and physico-chemical properties of new oxodiperoxomolybdenum complexes with nicotinic acid

Anna Szymańska [a], Wojciech Nitek [b], Dariusz Mucha [a], Robert Karcz [a], Katarzyna Pamin [a], Jan Połtowicz [a], Wiesław Łasocha [a,b,*]

[a] Jerzy Haber Institute of Catalysis and Surface Chemistry PAS, Niezapominajek 8, 30-239 Krakow, Poland
[b] Faculty of Chemistry, Jagiellonian University, Ingardena 3, 30-060 Krakow, Poland

ARTICLE INFO

Article history:
Received 8 February 2013
Accepted 4 May 2013
Available online 21 May 2013

Keywords:
Peroxo complex
Molybdates
Thermal decomposition
X-ray diffraction
Catalysis

ABSTRACT

Three new oxodiperoxomolybdenum complexes with nicotinic acid have been synthesized and characterized with the use of single-crystal analysis, XRPD versus temperature, TG/DSC, SEM and IR spectroscopy. The investigated compounds are: **1** – $(NH_4)_2{\cdot}[MoO(O_2)_2.N\text{-}nicO]_2$, **2** – $(nicH)_2{\cdot}[MoO(O_2)_2.N\text{-}nicO]_2{\cdot}2(H_2O)$, **3** – $MoO(O_2)_2(H_2O)nicH$; (N-nicO, nicH – denote nicotinic acid N-oxide and protonated nicotinic acid, respectively). Compounds **1, 2** are salts of the same acid with cyclic dinuclear anions, whereas compound **3** can be regarded as an inner salt. Compounds **1–3** are stable in ambient conditions, the respective percentages of oxygen in peroxo groups are 19.21%, 14.06% and 20.19%, respectively. Above 125 °C peroxo compounds **1–3** decompose, forming nanometric MoO_2 and MoO_3. TG/DSC curves reveal clear effects connected with the release of oxygen and strong exothermic effects connected with final loss of organic components. All the investigated complexes were found to be active in the oxidation of cyclooctane to cyclooctanone and cyclooctanol with molecular oxygen.

1. Introduction

Peroxo complexes with transition metals are an interesting group of compounds, important in the processes of catalytic oxidation of alcohols and sulfides, epoxidation, effluent treatment, pyrotechnics, hydrometallurgy, medicine, etc. [1]. Molybdenum compounds and hydrogen peroxide are significant substrates used in the design and syntheses of catalysts for "cleaner industrial processes" [2]. It is known that oxodiperoxometallates (Mo,W) are promising catalysts in adipic acid production through cyclohexene, cyclohexanol, cyclohexanone and 1,2-cyclohexanediol oxidation with H_2O_2 [3]. Thus, such catalysts are important in nitrogen oxide emission abatement.

Peroxo compounds containing organic ligands exhibit different activity in the processes of oxidation, as well as variable thermal stability. Proper selection of organic ligand enables the deposition of molecules containing peroxo groups on different carriers such as polymers.

When looking for new promising ligands, our attention was drawn to pyridine derivatives with a carboxyl side chain, due to well known chelating properties of such compounds. What is more, peroxo compounds with picolinic acid (2-carboxypyridine acid) are known and were found to be active in reaction of catalytic oxidation of alcohols [4]. Also certain peroxo compounds of Mo with nicotinic acid (3-carboxypyridine acid) were described in the literature by Djordjevic et al. [5]. However, these compounds were characterized by UV–Vis, IR spectroscopy and ^{1}H NMR measurements only. The compounds described in the literature have not been investigated either by X-ray or TG/DSC. Moreover, following published procedures [5] we could obtain neither suitable single crystals nor pure phases to perform structural powder diffraction studies. Thus, we have decided to re-examine synthesis procedures and properties of peroxomolybdates containing nicotinic acid.

The molecular structures of pyridine and carboxypyridine peroxomolybdenum compounds known so far are presented and discussed below.

1.1. Review of structures of similar compounds

In Crystal Structural Database CSD [6], 7 types of peroxomolybdates with pyridine, methylpyridine and pyridine-carboxylic acids have been found. In Scheme 1 their structures are presented (labelled by refcodes from CSD).

Among compounds presented above, all but one (OXPCXM) are oxodiperoxocomplexes. There are mononuclear as well as dinuclear compounds (PYPOMO10, PYPOAM10, MOHFUL), ionic salts or materials composed of molecules with no charge (LEHZIN, ICIVUL,

* Corresponding author at: Faculty of Chemistry, Jagiellonian University, Ingardena 3, 30-060 Krakow, Poland. Tel.: +48 126632053; fax: +48 126340515.
E-mail address: lasocha@chemia.uj.edu.pl (W. Łasocha).

0277-5387/$ - see front matter © 2013 Elsevier Ltd. All rights reserved.
http://dx.doi.org/10.1016/j.poly.2013.05.020

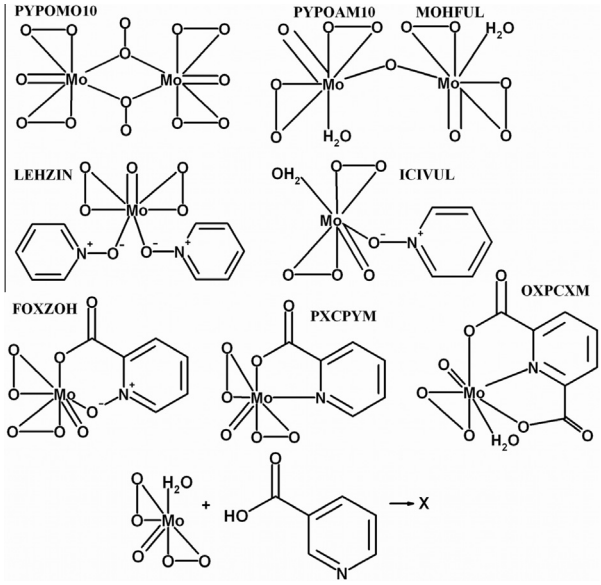

Scheme 1. Molecular structures of known peroxomolybdates with pyridine (1st row), pyridine N-oxides (2nd row), pyridine carboxylic acids (3rd row). Cations, if present, were omitted for clarity (N^+–O^- represent N-oxide fragment). In the bottom row reaction of the hypothetical reagent 'oxodiperoxomolybdenum' moiety with nicotinic acid is presented. X represents an unknown product.

OXPCXM). There are compounds containing "purely inorganic peroxomolybdate" anions (PYPOMO10, MOHFUL) and compounds composed of: pyridine N-oxides (LEHZIN, ICIVUL), pyridine-carboxylic acid (PXCPYM, OXPCXM) or pyridine carboxylic acid N-oxide molecules (FOXZOH). Picolinic acid (pyridine-2-carboxylic), an isomer of nicotinic acid, can act as a co-creator of "picolinic acid peroxomolybdate complex" and its molecules can undergo protonation acting as cations (PXCPYM).

Study of peroxomolybdenum nicotinic acid compounds can supplement the existing knowledge of peroxomolybdates with pyridine-carboxylic acids. Due to the different position of the carboxyl group (3-carboxopyridine acid), we can expect a new type of compounds, including multimeric (dimers, trimers, etc.) or polymeric anions (see Scheme 1). Review of the structures indicate that the results of syntheses with the use of nicotinic acid are difficult to predict and they are also interesting from the crystal engineering point of view.

2. Experimental

2.1. Materials

All chemicals were purchased from POCH Gliwice and Aldrich, were used as received.

2.2. Syntheses

Yellow crystals of **1, 2** were obtained initially from aqueous solutions of **HMA** (amonium **h**epta**m**olybd**a**te tetrahydrate $[(NH_4)_6Mo_7O_{24}{\cdot}4H_2O]$) with the addition of H_2O_2 and nicotinic acid. Since the synthesis was slow (several weeks) and not reproducible, we conducted extensive research to find fast and reliable methods of synthesis. Compounds **1, 2** were found to contain N-oxide groups (formed by oxidation of nicotinic acid); therefore, the use of nicotinic acid N-oxide in the synthesis process was attempted. In the course of preparatory work, reliable methods of synthesis of both compounds were elaborated. In addition, the compound **3** was isolated and examined.

Ammonium bis(pyridine-3-carboxylicacid N-oxide)bis{oxodiperoxomolybdate(VI)} compound **1. HMA** (1.43 mmol) was dissolved in cold H_2O_2 (30 ml, 30%, temp. ~0 °C). 1 ml of NH_3aq was added to the resulting solution. Next the blood-red solution was acidified with concentrated HCl until it turned yellow. During constant stirring of the solution 0.01 mol of nicotinic acid was added. After about 5–7 h the precipitate **A** was filtered off. The resulting solution was allowed to crystallize and after 3–4 days crystals of **1** were obtained. When nicotinic acid was replaced by nicotinic acid N-oxide, precipitate **1** was obtained after about 24 h. Yield 90%, C 21.43 (calc. 21.70), H 2.535 (calc. 2.43), N 8.61 (calc. 8.44).

Pyridinium-3-carboxylicacid bis(pyridine-3-carboxylicacid N-oxide)bis{oxodiperoxomolybdate(VI)} dihydrate, compound **2.** $Na_2MoO_4{\cdot}H_2O$ (0.01 mol) was dissolved in 30 ml (30%) cold H_2O_2. The resulting red solution was acidified by drops of HCl until it turned yellow. Next 0.02 mol of nicotinic acid was added to the solution. After 5–7 h the precipitate **B** was filtered off and the solution was left to crystallize at room temperature. After 5–7 days yellow crystals of **2** were obtained. Using a mixture of nicotinic acid N-oxide and nicotinic acid (1:1) the synthesis time is reduced to 1–2 days and the yield is increased. Yield 82%, C 29.69 (calc. 31.60), H 2.532 (calc. 2.65), N 5.70 (calc. 6.14).

Aquaoxodiperoxo(pyridinium-3-carboxylato)molybdenum(VI), compound **3**. **HMA** (1.23 g) was dissolved in hydrogen peroxide (20 ml). Next 0.01 mol of nicotinic acid was added (0.12 g) and the solution was left to crystallize. Small white crystals appeared after about one hour and the next day they were filtered off. Yield 80%, C 22.76 (calc. 22.73), H 22.50 (calc. 2.23), N 4.41 (calc. 4.42).

Crystals of **3** turned out to be the same compound as precipitate **B** obtained in previous procedure, whereas precipitate **A** is slightly different despite almost the same composition.

2.3. X-ray crystallographic study

Single-crystal X-ray diffraction studies were performed for all **1–3** compounds. Single crystals were picked up from mother solutions and mounted on the goniometer head. The temperature of the crystals during the measurement was 293 K. X-ray data were collected on a Bruker-Nonius Kappa-CCD diffractometer. For absorption correction the multiscan procedure was performed by diffractometer software [7]. Structure solution and refinement were carried out using the SHELXS and SHELXL-97 programs [8]. All non-hydrogen atoms were refined anisotropically. Hydrogen atoms were located from difference Fourier maps. Crystal data for all obtained oxodiperoxo complexes are presented in Table 1.

2.4. Measurements

For IR measurements the samples were pressed into pellets with KBr and investigated at room temperature with the use of Fourier and the vacuum spectrometer Bruker VERTEX 70 V. All spectral lines expected for oxodiperoxo compounds were found in the recorded spectra.

X-ray thermal decomposition studies were carried out using a powder diffractometer Philips X'Pert Pro MPD, equipped with an Anton Paar high-temperature chamber. X-ray data were collected at the following temperatures: 25, 50, 75, 100, 125, 150, 175, 200, 225, 250, 275, 300, 350, 400, 500, 600 and 25 °C again. The heating rate was 5 °C/min, the time of each measurement 15 min. Prior to measurement the temperature was stabilized for 5 min. The 2θ range was from 5 to 65°.

SEM images were performed for each sample after thermal decomposition (600 °C) with the use of an ultrahigh-resolution Field Emission Scanning Electron Microscope JEOL JSM-7500F

Table 1
Summary of crystal data of the investigated compounds.

	Compound **1**	Compound **2**	Compound **3**
Chemical formula	$C_{12}H_{16}Mo_2N_4O_{16}$	$C_{24}H_{24}Mo_2N_4O_{22}$	$C_6H_7MoNO_8$
Structural formula	$(NH_4)_2{\cdot}[MoO(O_2)_2C_5H_4NOCOO]_2$	$(C_5H_4NHCOOH)_2{\cdot}[MoO(O_2)_2C_5H_4NOCOO]_2{\cdot}2(H_2O)$	$MoO(O_2)_2(H_2O)\ C_5H_4NHCOO$
MW (g/mol)	664.1562	912.3482	317.0635
T (K)	293(2)	293(2)	293(2)
Wavelength Mo Kα (Å)	0.71073	0.71073	0.71073
Crystal system, SG	triclinic, $P\bar{1}$	monoclinic, $P2_1/c$	monoclinic, Pc
Cell parameters			
a (Å)	6.687(4)	7.504(2)	5.416(3)
b (Å)	6.965(4)	28.473(7)	5.350(2)
c (Å)	12.012(7)	7.777(2)	16.976(7)
α (°)	76.42(4)	90	90
β (°)	77.43(4)	111.43(1)	106.23(3)
γ (°)	69.48(4)	90	90
V (Å^3)	503.66(5)	1546.82(7)	472.29(5)
Z, Calculated density (g/cm^3)	1, 2.189	2, 1.955	2, 2.230
Absorption coefficient (mm^{-1})	1.344	0.916	1.42
F(000)	326	908	312
Crystal size (mm)	0.15 × 0.10 × 0.04	0.20 × 0.20 × 0.10	0.09 × 0.07 × 0.02
θ range	3.17–27.44	2.86–27.47	2.50–27.39
Limiting indices	$-8 \leqslant h \leqslant 8$, $-9 \leqslant k \leqslant 8$, $-15 \leqslant l \leqslant 15$	$-9 \leqslant h \leqslant 9$, $-36 \leqslant k \leqslant 35$, $-10 \leqslant l \leqslant 10$	$-7 \leqslant h \leqslant 6$, $-6 \leqslant k \leqslant 6$, $-20 \leqslant l \leqslant 21$
Reflections collected/unique	4180/2278 [R_{int} = 0.0504]	6124/3477 [R_{int} = 0.0249]	7688/2086 [R_{int} = 0.0606]
Completeness to theta	27.44, 99.3%	27.47, 98.2%	27.39, 100%
Absorption correction	multi-scan	multi-scan	multi-scan
Maximum and minimum transmission	0.9482 and 0.8238		0.3577 and 0.1735
Refinement method	full-matrix least-squares on F^2	full-matrix least-squares on F^2	full-matrix least-squares on F^2
Data/restraints/parameters	2278/6/171	3477/4/253	2086/2/94
Goodness of fit on F^2	1.098	0.999	1.583
Final R indices [$I > 2\sigma(I)$]	R_1 = 4.59, wR_2 = 11.04	R_1 = 2.89, wR_2 = 6.35	R_1 = 4.37, wR_2 = 10.47
R indices (all data)	R_1 = 6.87, wR_2 = 10.32	R_1 = 4.20, wR_2 = 6.64	R_1 = 5.10, wR_2 = 11.90
Extinction coefficient	0.008(2)	0.0015(3)	0.000(2)
Largest difference peak and hole (eÅ^{-3})	2.036 and −0.749	0.457 and −0.579	1.258 and −1.854
CCDC	848660	866614	848773

equipped with an INCA PentaFETx3 EDS system and a K575X Turbo Sputter Coater.

TG/DSC measurements were performed using a NETZSCH STA 409 Luxx instrument, at a heating rate of 25°/min in an air atmosphere. The temperature range was from 30 to 1000 °C.

2.5. Catalytic activity

The oxidation of cyclooctane was performed in a stainless steel batch reactor system at 393 K and under the air pressure of 10 atm, with the cyclooctane-to-oxygen molar ratio set at 6.5. In a typical experiment, 60 ml of substrate containing the amount of catalyst providing a concentration of 3.3×10^{-4} M was introduced in the deaerated autoclave and the whole system was heated until a temperature of 393 K was reached. Air was then introduced and after 6 h the oxidation products were analyzed by an Agilent 6890 N Gas Chromatograph equipped with an Innowax (30 m) column. The yield values were verified by addition of an internal standard, chlorobenzene, at the end of the reaction.

3. Results and discussion

3.1. Crystal structure data

Crystal data are summarized in Table 1. Molecular structures for the compounds **1–3** are presented in Figs. 1–3. The figures were drawn using the Diamond software package [9]. List of essential distances and angles are presented in Table 2 and in Table 3 hydrogen bonds are summarized.

Compounds **1** and **2** are salts of the same acid, with cyclic dinuclear centrosymmetric anions (Figs. 1a and 2a), therefore they will be described together. Compound **1** is an ammonium salt, whereas **2** is a hydrated salt with protonated nicotinic acid (nic-H) as cation. In both compounds nicotinic acid N-oxide (N-nicO), formed during synthesis, was found to be a building block of cyclic anions. In both compounds two O atoms bridging Mo with organic ligands forming cyclic dinuclear centrosymmetric anions were found. The bridging oxygen atoms are in *cis* position relative to each other. One bridging oxygen atom belongs to a carboxylic group, the second one to an N-oxide group.

As in most oxodiperoxomolybdenum complexes, in **1–2** the Mo atom is coordinated by seven oxygen atoms in the form of a pentagonal bipyramid. In the pentagonal plane two peroxo groups are placed (average O–O is 1.475 Å). In each compound one apical terminal oxygen atom (M=O ~1.675 Å) is observed. The Mo1 atom is shifted from the pentagonal plane (created by atoms O2, O4–O5, O6–O7) by 0.362 and 0.355 Å, respectively in compounds **1** and **2**. Also an angle between pentagonal plane and pyridine ring (N1–C6) in both compounds is almost the same (37°).

In both compounds nicotinic acid N-oxide fragments from adjacent anions, form a system of molecules interacting by π−π face-to-face stacking (distances between interacting atoms ~3.5 Å (see Figs. 1b and 2b)). Additionally, in compound **2** one can also find infinite columns of twisted nicotinic acid molecules (forming cations) interacting by 'face-to-face' stacking. These columns are oriented along [0 0 1], the shortest distance between N21···C24[x, $-0.5 - y$, $-0.5 + z$] atoms is 3.406 Å (see Fig. 2b). Hydrogen bonds between NH_4^+ and oxygens from cyclic anions in compound **1**, form complex three-dimensional structure. The anions and water

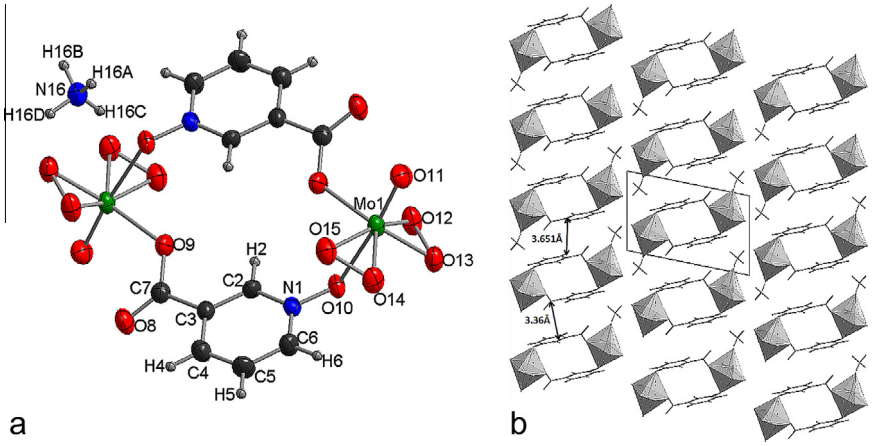

Fig. 1. Asymmetric unit (a) and packing of molecules (b) for compound **1**.

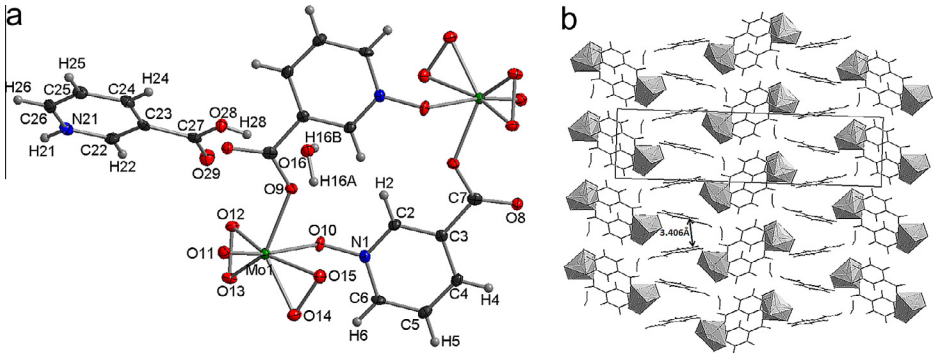

Fig. 2. Asymmetric unit (a) and packing of molecules (b) for compound **2**.

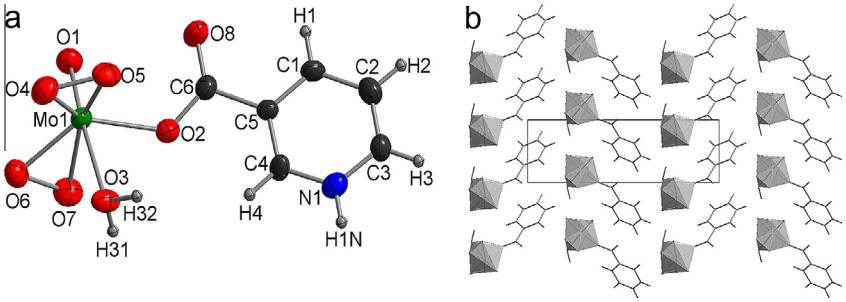

Fig. 3. Asymmetric unit (a) and packing of molecules (b) for compound **3**.

molecules in compound **2** form layers, joined together by hydrogen bonds with the protonated nicotinic acid molecules located in the space between the layers (Table 3, Figs. 1b and 2b).

A similar system created by picolinic acid N-oxide (N-picO) has already been studied [4]. Within that study, a compound containing N-picO connected to the Mo atom by two oxygens (from the carboxylato and N-oxide groups) was obtained (FOXZOH-Scheme 1). Due to the convenient mutual positions of these groups, an isolated monomeric molecules were obtained (please note that N-picO and N-nicO are chelating bidentate ligands). In the case of N-nicO (3-carboxypyridine-N-oxide) cyclic dinuclear anions are preferred.

Compound **3** is an inner salt. Fig. 3a presents its molecular structure with labeling scheme. The negative charge of the oxodiperoxomolybdate fragment is compensated by the positive charge of the protonated pyridine ring. In the pentagonal plane two peroxo groups (O4–O5, O6–O7) and one bridging O2 atom from the deprotonated carboxylic group are present. Two apical to the pentagonal plane positions are occupied by a water molecule O3, and a terminal oxygen atom O1. The Mo atom is moved from pentagonal plane by 0.402 Å, the pentagonal plane and pyridine ring are twisted by an angle 72.8°. Pyridine fragments arranged parallel to each other and forming columns along [1 0 0] interact through $\pi-\pi$ interactions. The shortest distance between N1···C1[−1 + *x*, *y*, *z*] atoms from adjacent rings is equal to 3.698 Å. Molecules linked by hydrogen bonds (Table 3) form isolated, two-dimensional layers parallel to the plane (0 0 1) (see Fig. 3b).

Our results indicate that 3 can be considered as an intermediate obtained initially in the process of formation of compounds **1** and **2**. Subsequently, nitrogen in the pyridine ring is oxidized to form an N-oxide group followed by condensation and formation of a cyclic dinuclear anion. This chemical reaction path is confirmed

Table 2
Selected bond lengths (Å) and angles (°) in investigated compounds.

Compound **1**		Compound **2**		Compound **3**	
Mo1—O11	1.672(3)	Mo1—O11	1.6766(16)	Mo1—O1	1.675(4)
Mo1—O14	1.924(3)	Mo1—O13	1.9332(16)	Mo1—O4	1.922(4)
Mo1—O13	1.932(3)	Mo1—O15	1.9370(17)	Mo1—O6	1.932(5)
Mo1—O15	1.942(3)	Mo1—O14	1.9443(17)	Mo1—O5	1.940(3)
Mo1—O12	1.956(3)	Mo1—O12	1.9462(16)	Mo1—O7	1.938(3)
Mo1—O9^{i}	2.073(3)	Mo1—O9	2.0613(16)	Mo1—O2	2.053(3)
Mo1—O10	2.311(3)	Mo1—O10^{i}	2.3095(16)	Mo1—O3	2.335(3)
O12—O13	1.473(5)	O14—O15	1.482(2)	O6—O7	1.469(5)
O14—O15	1.464(5)	O13—O12	1.478(2)	O4—O5	1.461(5)
N1—O10	1.338(4)	N1—O10	1.346(2)		
O11—Mo1—O14	102.12(16)	O11—Mo1—O13	100.96(7)	O1—Mo1—O4	104.32(19)
O11—Mo1—O13	102.68(16)	O11—Mo1—O15	103.28(8)	O1—Mo1—O6	102.82(14)
O14—Mo1—O13	89.61(15)	O13—Mo1—O15	133.09(7)	O4—Mo1—O6	89.31(18)
O11—Mo1—O15	101.56(17)	O11—Mo1—O14	103.17(8)	O1—Mo1—O5	103.3(2)
O14—Mo1—O15	44.51(14)	O13—Mo1—O14	90.70(7)	O4—Mo1—O5	44.46(16)
O13—Mo1—O15	131.69(15)	O15—Mo1—O14	44.91(7)	O6—Mo1—O5	131.21(18)
O11—Mo1—O12	101.80(17)	O11—Mo1—O12	102.00(7)	O1—Mo1—O7	102.3(2)
O14—Mo1—O12	131.90(16)	O13—Mo1—O12	44.80(7)	O4—Mo1—O7	130.91(16)
O13—Mo1—O12	44.51(14)	O15—Mo1—O12	154.18(7)	O6—Mo1—O7	44.62(16)
O15—Mo1—O12	156.38(15)	O14—Mo1—O12	132.25(7)	O5—Mo1—O7	153.99(14)
O11—Mo1—O9^{i}	96.05(15)	O11—Mo1—O9	94.07(7)	O1—Mo1—O2	96.85(19)
O14—Mo1—O9^{i}	128.51(14)	O13—Mo1—O9	133.31(7)	O4—Mo1—O2	129.68(18)
O13—Mo1—O9^{i}	132.53(14)	O15—Mo1—O9	84.10(7)	O6—Mo1—O2	129.7(2)
O15—Mo1—O9^{i}	84.90(14)	O14—Mo1—O9	128.47(7)	O5—Mo1—O2	86.61(15)
O12—Mo1—O9^{i}	89.25(14)	O12—Mo1—O9	88.99(7)	O7—Mo1—O2	86.26(16)
O11—Mo1—O10	172.57(14)	O11—Mo1—O10^{i}	171.40(7)	O1—Mo1—O3	174.65(17)
O14—Mo1—O10	84.39(13)	O13—Mo1—O10^{i}	81.06(6)	O4—Mo1—O3	80.48(14)
O13—Mo1—O10	80.75(13)	O15—Mo1—O10^{i}	80.81(6)	O6—Mo1—O3	79.39(17)
O15—Mo1—O10	80.49(13)	O14—Mo1—O10^{i}	85.09(7)	O5—Mo1—O3	78.33(13)
O12—Mo1—O10	75.89(13)	O12—Mo1—O10^{i}	73.44(6)	O7—Mo1—O3	75.73(13)
O9^{i}—Mo1—O10	76.95(12)	O9—Mo1—O10^{i}	78.72(6)	O2—Mo1—O3	78.11(14)
C7—O9—Mo1^{i}	125.0(3)	C7—O9—Mo1	128.68(15)	C6—O2—Mo1	127.0(3)
N1—O10—Mo1	122.5(2)	N1—O10—Mo1^{i}	120.20(13)		
Symmetry operations: (i) $1-x, 1-y, 1-z$;		Symmetry operations: (i) $2-x, -y, 1-z$.			

by the length of synthesis time. Compound **3** is formed within 1–2 h, while the syntheses of **1** and **2** salts require several days.

Compounds investigated by us show a great similarity to the group of mono- and dinuclear compounds formed with the participation of organo-phosphorus and arsenic ligands [10]. In both groups of compounds the metal center(s) have essentially identical pentagonal-bipyramidal coordination (with Me atom shifted ~0.4 Å from LS pentagonal plane). However, in the case of the compounds investigated by us only 'nonbonding η^2-peroxo groups' occur. In mentioned above heteropolyperoxometalates with P or As, each metal center contain one 'nonbonding η^2' peroxo group, whereas the other peroxo group is bonding η^1,η^2 [10].

In conclusion, we have found that using nicotinic acid some similarities with pyridine-based compounds were preserved. In particular, pyridine fragment can be oxidized or protonated and nicotinic acid N-oxide, protonated nicotinic acid, or both of them, could be present in obtained salts **1** and **2**.

We were not able to obtain compounds with a direct Mo–N bond, although by analogy with picolinic acid (PXCPYM) they might exist. However, we have synthesized compounds with molecular architecture as complex and intriguing as compounds with picolinic acid or pyridine. In particular, we have obtained not reported yet dinuclear, cyclic, centrosymmetric oxodiperoxomolybdate anions **1, 2** and an inner salt type compound **3**.

3.2. IR studies

The aim of IR studies was to verify the purity of investigated samples and their identification. An additional objective was to compare our results with those from previous spectroscopic studies [5]. Vibrations indicating the presence of oxo and peroxo groups with tentative assignments based on literature data [10,11] are collected in Table 4. The spectra of investigated compounds are shown in Fig. 4. Compounds **1** and **2** differ from the spectrum of **3** by the presence of bands around 490, 800 and 1200 cm^{-1}. According to the literature, these bands can be assigned to vibrations associated with the presence of N-oxide group.

The lack of complete IR spectra prevents a full comparison and reliable matching of our compounds with complexes described by Djordjevic et al. [5]. However, it seems that we have investigated similar compounds or mixtures thereof. The assignment of IR bands fully corresponding to the crystal data indicates the usefulness of IR investigations for identification purposes or in the case of poor-quality crystals.

3.3. Thermal decomposition

Thermal decomposition studies were performed to correlate thermal stability with molecular structure. XRPD versus temperature demonstrated the stability of **1, 2** (cyclic, compact anion, without water in Mo coordination sphere) up to 125–150 °C (Supplementary data, Figs. S1 and S2). Compound **3** (monomeric anion, H_2O coordinated to Mo atom) decomposes earlier around 100 °C (Supplementary data, Fig. S3). During degradation of compounds **1** and **3**, the amorphous phase can be observed up to 350 °C, after which molybdenum trioxide is formed. For compound **2** (much richer in organic, reducing components) degradation proceeds through the amorphous phase (125–175 °C) and then MoO_2 is formed at the temperature of 200 °C, which finally recrystallizes into MoO_3 (at a temperature around 275 °C).

Table 3
Hydrogen bonds with H···A < r(A) + 2.000 angstroms and <DHA> 110 deg.

D–H	d(D–H)	d(H···A)	<DHA	d(D···A)	A
*Compound **1***					
N16–H16A	0.932	2.179	166.60	3.093	O15[$x+1, y-1, z$]
N16–H16A	0.932	2.208	152.20	3.063	O14[$x+1, y-1, z$]
N16–H16B	0.928	2.180	145.86	2.994	O14[$-x+1, -y+1, -z$]
N16–H16B	0.928	2.326	122.80	2.935	O11[$x, y-1, z$]
N16–H16C	0.928	1.936	160.30	2.827	O10
N16–H16D	0.930	2.150	140.88	2.930	O13[$-x+2, -y+1, -z$]
N16–H16D	0.930	2.314	141.58	3.097	O12[$-x+2, -y+1, -z$]
N16–H16D	0.930	2.553	118.95	3.111	O13
*Compound **2***					
O16–H16A	0.926	1.869	176.40	2.794	O10[$-x+2, -y, -z+1$]
O16–H16B	0.919	1.996	163.43	2.888	O14[$x, y, z-1$]
O16–H16B	0.919	2.402	130.36	3.077	O15[$x, y, z-1$]
O28–H28	0.798	1.800	177.47	2.597	O16
N21–H21	0.860	1.917	174.76	2.774	O8[$x, -y-1/2, z-1/2$]
*Compound **3***					
N1–H1 N	0.860	2.174	136.96	2.863	O1[$x-1, y-1, z$]
N1–H1 N	0.860	2.231	136.69	2.917	O8[$x-1, y-1, z$]
O3–H32	0.881	1.917	154.67	2.739	O6[$x, y-1, z$]
O3–H32	0.881	2.293	165.33	3.153	O7[$x, y-1, z$]
O3–H31	0.862	2.139	154.09	2.939	O4[$x-1, y, z$]
O3–H31	0.862	2.212	153.36	3.008	O5[$x-1, y, z$]

Table 4
IR spectra vibrations and band assignments connected with oxodiperoxomolybdate [10,11] and nicotinic acid N-oxide moiety for compounds 1, 2 and 3*.

Vibrations/compounds	ν(M=O)	ν_{sym} (O–O)	ν_{asym} (M–(O)$_2$)	ν_{sym} (M–(O)$_2$)	(N-oxide) vibrations
1	970vs, 948vs	893w, 874s, 856vs	581s, 567m	543w, 534w	818m, 799s, 489m
2	970s, 948vs	891w, 872s, 856vs,	579m, 569m,	551w, 537w	827w, 824w, 800m, 490m
3	967vs	871m, 860vs, 841w	576s	547m	–
$Me_2\{O[MoO(O_2)_2H_2O]_2\}$ [11]	963–970s 940–943s	840–891	568–607	526–559	–

* Intensity symbols: vs-very strong; s-strong; m-medium; w-weak.

3.4. SEM investigations

Before heat treatment, investigated compounds form characteristic crystalline blocks with smooth surfaces and sharp edges. Their SEM images are typical for crystalline materials. SEM images of materials after thermal decomposition (Fig. 5) show that samples **1–3** annealed to 600 °C are forming agglomerates in the shape of rounded rectangular plates ($\sim 1 \times 10$ μm) with thicknesses of 0.15–0.25 μm.

3.5. TG/DSC studies

TG/DSC curves should indicate obvious correlations with X-ray thermal decomposition studies. However, differences in heating rate and time of the measurements result in a shift towards lower temperatures in the case of thermal XRPD investigations.

Compound **1**. Analysis of TG/DSC curves (Supplementary data, Fig. S4) indicates that investigated compound decomposes in the exothermic process around 200 °C, with a great loss of mass corresponding to the organic part and oxygen from peroxo groups. At a temperature range 200–300 °C unknown phase prevails, with nominal composition $(NH_4)_2MoO_4$ or $H_2MoO_4{\cdot}H_2O$ (this cannot be verified due to amorphous XRPD patterns). At about 500 °C MoO_3 is formed, which agrees with thermal decomposition analysis (Supporting materials, Fig. S4). The melting point of molybdenum trioxide is observed around 795 °C.

Compound **2**. The first mass loss at around 150 °C can be correlated with the loss of two water molecules and two molecules of O_2 (observed 11.29%, calculated 10.97%) (Supporting materials, Fig. S5). Around 240 °C the next mass loss is observed, corresponding to the loss of two nicotinic acid molecules (calculated 27.18%, observed 27.82%). The third decrease in sample mass is observed over a wide range of temperatures 300–600 °C and is possibly correlated to the disconnection of two other molecules of nicotinic acid accompanied by reduction of MoO_3 to MoO_2. In the case of formation of MoO_3 or MoO_2 as final decomposition products, the total mass loss would be 68.43% or 73%, respectively. As one can find from TG/DSC data (Supporting materials, Fig. S5), total mass loss is ~75%, which clearly confirm MoO_2 formation. The results of TG/DSC studies are in agreement with XRPD versus temperature investigations, which also indicate MoO_2 formation.

Compound **3.** First mass loss is correlated with disconnection of oxygen molecule O_2 (150 °C, calculated 10.1, observed 11.38%). (Supporting materials, Fig. S6). The next stages of decomposition are not easy to interpret: in the case of good separation we should be able to observe a loss of water molecule equaling 5.67% and loss of organic part of 39.15%. Total mass loss reaches up 43.72% at temperature range 170–500 °C, which agrees with degradation to MoO_3 (calculated 44.51%). At 795 °C the melting point of MoO_3 is observed.

The authors of recently published work [12] indicated that the process of thermal decomposition of compounds such as $[MoO(O_2)_2(L)]$ may depend on the donor–acceptor character of the ligand L. Our results indicate that the situation may be even more complex. Compounds **1–3** have been well characterized by XRD methods (crystal structure and phase analysis). **1** and **2** are similar, because both compounds are salts of the same acid. However, when TG/DSC studies are taken into account, compounds **2**

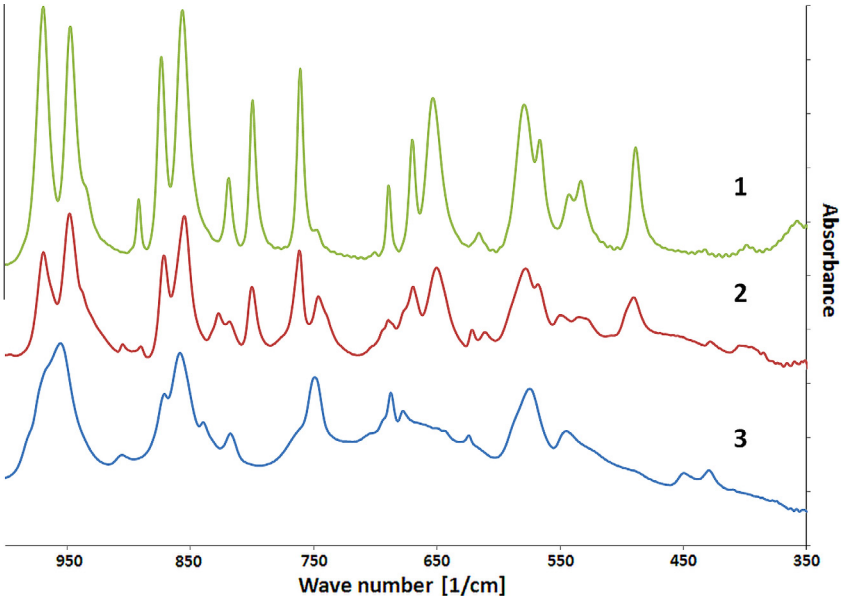

Fig. 4. IR spectra of compounds **1–3**.

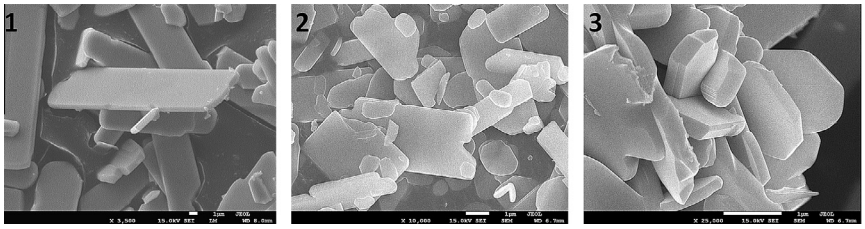

Fig. 5. SEM images of compounds after annealing in 600 °C.

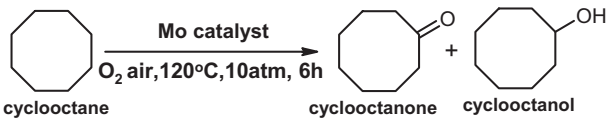

Scheme 2. Oxidation of cyclooctane with molybdenum oxodiperoxo complex.

Table 5
Cyclooctane oxidation with the use of molybdenum oxodiperoxo complexes.

	Ketone Yield (%)[a]	Alcohol Yield (%)[a]	Ketone + Alcohol Yield (%)[a]	Ketone/ Alcohol ratio
Compound **1**	32.9	20.2	53.1	1.6
Compound **2**	33.9	18.5	53.4	1.8
Compound **3**	24.8	16.7	41.5	1.5
MoO_3	3.4	2.4	5.8	1.4
Cobalt isooctanate	30.7	9.1	39.8	3.4

[a] Calculated on the basis of oxygen quantity in batch reactor.

and **3** are more similar. Compound **1** is the most heat-resistant (Supporting materials, Fig. S4) – the first mass loss is observed at around 200 °C – whereas for **2** and **3** the first mass losses are around 125–150 °C. The only reasonable explanation of this fact involves the type of cations and their surroundings. **1** contains ammonium cations which are resistant to oxidation, whereas in compounds **2** and **3** organic cations (strong reductors) are placed close to oxodiperoxomolybdate anions (very strong oxidizers). However, our explanation is only a working, qualitative hypothesis and we agree with the authors of work [12], that additional extensive experimental study is needed to explain the phenomenon of thermal decomposition of diperoxocompounds.

4. Catalytic activity

We have examined the catalytic activity of oxodiperoxomolybdenum complexes in the oxidation of cyclooctane to cyclooctanone and cyclooctanol with molecular oxygen (Scheme 2).

Results of the catalytic investigations are summarized in Table 5. All the investigated peroxocomplexes with nicotinic acid were active in the process of cyclooctane oxidation. The structures of oxodiperoxomolybdenum catalysts **1** and **2** are similar and exhibit almost the same catalytic activity and selectivity. These cyclic complexes **1** and **2**, both built of two oxodiperoxo and two N-nicO fragments, are more active than a simple oxodiperoxomolybdenum complex **3**. What is more, molybdenum trioxide (PDF 04-08-4311), which contains only oxo oxygens, exhibits poor activity in oxidation of cyclooctane. Also, catalytic activity of nicotinic acid N-oxide (N-nicO) is negligible. Thus, only the simultaneous presence of peroxo groups and an organic ligand (N-oxide) causes a significant increase in the catalytic activity. This conclusion is supported by almost identical geometric parameters of oxodiperoxo moieties in anions of **1–3** (bond lengths Mo═O,<O–O>, Mo < O2, details see Table 2).

For comparison, oxidation of cyclooctane in the presence of industrial catalyst cobalt isooctanate, used in Cyclopol process [13–15] (cyclohexane oxidation), was performed. Catalytic activity

(measured as total cyclooctane conversion) of oxodiperoxomolybdenum complexes is higher than in the case of the industrial catalyst (Table 5). The following order of catalytic activity was obtained: **2** $C_{24}H_{24}N_4O_{10}\{O[MoO(O_2)_2]\}_2$ > **1** $C_{12}H_{12}N_4O_4\{O[MoO(O_2)_2]\}_2$ > **3** $C_6H_5NO_2\{MoO(O_2)_2(H_2O)\}$ > Co(isooctanate) ≫ MoO_3. Although industrial catalyst is much more selective in process of ketone production, the obtained results indicate that the tested peroxo-compounds **1–3** are promising catalysts in oxidation with molecular oxygen.

5. Conclusions

Three new oxodiperoxomolybdates with nicotinic acid were synthesized. Characteristic common feature of compounds **1** and **2** is the presence of cyclic dinuclear anion containing a pyridine N-oxide moiety. Formed in the early stages of the synthesis compound **3** seems to be an intermediate product preceding the formation of compounds **1** and **2**. All compounds are stable at room temperature, above 100–125 °C they decompose through amorphous phase and at higher temperatures crystals of MoO_2 or MoO_3 appear.

Investigated compounds were found to be active in reaction of the cyclooctane oxidation. The highest activity was observed in the case of compounds **1** and **2**. Activity of investigated peroxo compounds **1–3** was greater than in the case of commercial catalyst used in cyclohexane oxidation. Catalytic activity seems to be synergistic effect of the simultaneous presence of peroxomolybdenum and N-oxide moieties. Similar behavior of catalytic activity was observed earlier in the case of peroxomolybdenum complexes with picolinic acid [4]. Our studies resolved also an old scientific dilemma concerning the existence of certain peroxomolybdenum–nicotinic acid complexes [5].

Acknowledgements

The research has been partly supported by the EU Human Capital Operation Program, Polish Project No. POKL.04.0101-00-434/08-00. The X-ray research was carried out with equipment purchased thanks to the financial support of the European Regional Development Fund within the framework of the Polish Innovation Economy Operational Program (contract no. POIG.02.01.00-12-023/08).

Appendix A. Supplementary data

CCDC 848660, 866614, 848773 contains the supplementary crystallographic data for **1**–**3**, respectively. These data can be obtained free of charge via http://www.ccdc.cam.ac.uk/conts/retrieving.html, or from the Cambridge Crystallographic Data Centre, 12 Union Road, Cambridge CB2 1EZ, UK; fax: (+44) 1223 336 033; or e-mail: deposit@ccdc.cam.ac.uk. Supplementary data associated with this article can be found, in the online version, at http://dx.doi.org/10.1016/j.poly.2013.05.020.

References

[1] J. Nasrin, M.S. Islam, J. Appl. Sci. 7 (4) (2007) 597.
[2] W.R. Sanderson, Pure Appl. Chem. 72 (7) (2000) 1289.
[3] W. Zhu, H. Li, X. He, Q. Zhang, H. Shu, Y. Yan, Catal. Commun. (2008) 551.
[4] O. Bortolini, S. Campestrini, F. Di Furia, G. Modena, G. Valle, J. Org. Chem. 52 (24) (1987) 5467.
[5] C. Djordjevic, B.C. Puryear, N. Vuletic, C.J. Abelt, S.J. Sheffield, Inorg. Chem. 2 (1988) 2926.
[6] Cambridge Structural Database (2011, v. 2), REFCODES used in this paper:;
(a) FOXZOH, see reference [4];
(b) ICIVUL F.R. Sensato, Q.B. Cass, E. Longo, J. Zukerman-Schpector, R. Custodio, J. Andres, M.Z. Hernandes, R.L. Longo, Inorg. Chem. 40 (2001) 6022;
(c) . LEHZINW.P. Griffith, A.M.Z. Slawin, K.M. Rhompson, D.J. Williams, Chem. Commun. (1994) 569;
(d) . MOHFULM. Grzywa, W. Nitek, W. Łasocha, J. Mol. Struct. 888 (2008) 318;
(e) . OXPCXM, PXCPYMS.E. Jacobson, R. Tang, F. Mares, Inorg. Chem. 17 (1978) 3055;
(f) . PYPOMO10, PYPOAM10J.-M. Le Carpentier, A. Mitschler, R. Weiss, Acta Crystallogr. (1972) 1288.
[7] MULTISCAN R.H. Blessing, Acta Crystallogr. A51 (1995) 33.
[8] G.M. Sheldrick, SHELXS-97, SHELXL-97, University of Göttingen, Germany, 1997.
[9] K. Brandenburg, Diamond version 3.2g, Crystal Impact GbR, Bonn, Germany, 1997–2001.
[10] N.M. Gresley, W.P. Griffith, B.C. Parkin, A.J.P. White, D.J. Williams, J. Chem. Soc., Dalton Trans. (1996) 2039.
[11] M. Grzywa, W. Nitek, W. Łasocha, J. Mol. Struct. 919 (2009) 59.
[12] T.T. Bhengu, D.K. Sanyal, Termochim. Acta 397 (2003) 181.
[13] R. Pohorecki, W. Moniuk, P.T. Wierzchowski, Chem. Eng. Res. Des. 87 (2009) 349.
[14] Patent Pl nr 205510 B1.
[15] Patent Pl nr 209834 B1.